

# A dynamic eddy-viscosity model based on the invariants of the rate-of-strain

By R. W. C. P. Verstappen<sup>†</sup>, S. T. Bose, J. Lee<sup>‡</sup>, H. Choi<sup>¶</sup> AND P. Moin

Large-eddy simulation (LES) seeks to predict the dynamics of spatially filtered turbulent flows. By construction, the LES solution contains only scales of size  $\geq \Delta$ , where  $\Delta$  denotes some user-chosen length scale of the spatial filter. A large-eddy simulation based on an eddy-viscosity model and a Navier-Stokes simulation differ only in diffusion coefficient. Therefore, we focus on the question: “When does eddy diffusivity reduce a turbulent flow to eddies of size  $\geq \Delta$ ?”. It is deduced that the eddy viscosity  $\nu_e$  has to depend on the two invariants  $q$  and  $r$  of the filtered rate-of-strain tensor. We present a dynamic version of the resultant eddy-viscosity model and present results from LES of isotropic turbulence and turbulent channel flow.

## 1. Problem setting

The Navier-Stokes equations provide an appropriate model for turbulent flow. In the absence of compressibility ( $\nabla \cdot u = 0$ ), the equations are

$$\partial_t u + (u \cdot \nabla)u + \nabla p = 2\nu \nabla \cdot S(u), \quad (1.1)$$

where  $u$  is the fluid velocity field,  $p$  stands for the pressure,  $\nu$  denotes the viscosity, and  $S(u) = \frac{1}{2}(\nabla u + \nabla u^T)$  is the symmetric part of the velocity gradient. Turbulent flows can generally not be computed directly from Eq. (1.1) because the solution  $u$  possesses length scales that cannot be feasibly resolved numerically. Therefore, numerical simulations of turbulence have to resort to models of the effects of the small scales of motion on the large, energy-containing scales that are resolved. Formally, large-eddy simulation (LES) seeks to predict the dynamics of spatially filtered flows. If a spatial filter  $u \mapsto \bar{u}$  is applied to Eq. (1.1) an expression depending on both the full velocity field  $u$  and the filtered field  $\bar{u}$  results, due to the nonlinearity. The dependence on  $u$  can be removed by adopting an eddy-viscosity model, for example. The governing equation is then given by

$$\partial_t v + (v \cdot \nabla)v + \nabla p = 2\nabla \cdot ((\nu + \nu_e) S(v)), \quad (1.2)$$

where  $\nu_e$  denotes the eddy viscosity, and  $v$  is supposed to approximate the filtered Navier-Stokes solution  $\bar{u}$ .

The very essence of large-eddy simulation is that  $v$  contains only eddies of size  $\geq \Delta$ , where  $\Delta$  denotes the user-chosen length of the filter. This property enables us to solve Eq. (1.2) numerically when it is not feasible to compute the full turbulent flow field  $u$ . Eq. (1.2) is formally equivalent to the Navier-Stokes equations with a modified diffusion coefficient; hence, the desired effect is to eliminate all scales of size  $< \Delta$ . Therefore, we view the eddy viscosity as a function of  $v$  that is to be determined such that the

<sup>†</sup> Johann Bernoulli Institute for Mathematics and Computer Science, University of Groningen, Netherlands

<sup>‡</sup> School of Mechanical and Aerospace Engineering, Seoul National University

dynamically significant scales of motion in the solution  $v$  of Eq. (1.2) are greater than (or equal to)  $\Delta$ .

## 2. When does eddy diffusivity counteract the production of subfilter scales sufficiently?

We consider an arbitrary part  $\Omega_\Delta$  with characteristic length  $\Delta$  of the flow domain and take the filtered velocity  $\bar{v}$  equal to the average of  $u$  over  $\Omega_\Delta$ ; this filter is known as a box or top-hat filter. Furthermore, we suppose that  $\Omega_\Delta$  is a periodic box, so that boundary terms resulting from integration by parts (in the computations to come) vanish. Poincaré's inequality states that there exists a constant  $C_\Delta$ , depending only on  $\Omega_\Delta$ , such that for every  $v$ ,

$$\int_{\Omega_\Delta} \|v - \bar{v}\|^2 dx \leq C_\Delta \int_{\Omega_\Delta} \|\nabla v\|^2 dx. \quad (2.1)$$

The optimal constant  $C_\Delta$ , the Poincaré constant for the domain  $\Omega_\Delta$ , is the inverse of the smallest (non-zero) eigenvalue of the dissipative operator  $-\nabla^2$  on  $\Omega_\Delta$ . It is given by  $C_\Delta = (\Delta/\pi)^2$  for convex domains  $\Omega_\Delta$  (Payne & Weinberger 1960).

The residual field  $v' = v - \bar{v}$  contains eddies of size smaller than  $\Delta$ . The eddy viscosity must keep them from becoming dynamically significant. Poincaré's inequality (2.1) shows that the  $L^2(\Omega_\Delta)$  norm of the residual field  $v'$  is bounded by a constant (independent of  $v$ ) times the  $L^2(\Omega_\Delta)$  norm of  $\nabla v$ . Consequently, we can confine the dynamically significant part of the motion to scales  $\geq \Delta$  by damping the velocity gradient with the help of an eddy viscosity. To see how the evolution of the  $L^2(\Omega_\Delta)$  norm of  $\nabla v$  is to be damped, we consider the residual field  $v'$  first:

$$\frac{d}{dt} \int_{\Omega_\Delta} \frac{1}{2} \|v'\|^2 dx = -\nu \int_{\Omega_\Delta} \|\nabla v'\|^2 dx + \int_{\Omega_\Delta} T(\bar{v}, v') dx - \nu_e \int_{\Omega_\Delta} \|\nabla v'\|^2 dx.$$

Here,  $\int_{\Omega_\Delta} T(\bar{v}, v') dx$  represents the energy transfer from  $\bar{v}$  to  $v'$ . Obviously, the energy of  $v'$  has to decrease quickly, since Eq. (1.2) should not produce subfilter scales. Now suppose that the eddy viscosity is taken such that the last two terms in the right-hand side above cancel each other out. Then we have

$$\frac{d}{dt} \int_{\Omega_\Delta} \frac{1}{2} \|v'\|^2 dx = -\nu \int_{\Omega_\Delta} \|\nabla v'\|^2 dx. \quad (2.2)$$

This equation shows that the evolution of the energy of  $v'$  is not depending on  $\bar{v}$ . Stated otherwise, the energy of subfilter scales dissipates at a natural rate, without any forcing mechanism involving scales larger than  $\Delta$ . With the help of the Poincaré inequality (2.1) and the Gronwall's lemma, we obtain from Eq. (2.2) that the energy of the subfilter scales,  $\int_{\Omega_\Delta} \|v'\|^2(x, t) dx$ , decays at least as fast as  $\exp(-2\nu t/C_\Delta)$ , for *any* filter length  $\Delta$ . Applying Poincaré's inequality and Gronwall's lemma to

$$\frac{d}{dt} \int_{\Omega_\Delta} \frac{1}{2} \|\nabla v\|^2 dx = -\nu \int_{\Omega_\Delta} \|\nabla^2 v\|^2 dx \quad (2.3)$$

results into the same rate of decay:

$$\int_{\Omega_\Delta} \|v'\|^2(x, t) dx \stackrel{(2.1)}{\leq} C_\Delta \int_{\Omega_\Delta} \|\nabla v\|^2(x, t) dx \stackrel{(2.3)}{\leq} C_\Delta e^{-2\nu t/C_\Delta} \int_{\Omega_\Delta} \|\nabla v\|^2(x, 0) dx.$$

So, we can keep the subfilter component  $v'$  under control with the help of Eq. (2.3). The

(minimum) amount of eddy viscosity needed to satisfy the dissipative condition (Eq. 2.3) can be derived by taking the  $L^2$  innerproduct of Eq. (1.2) with  $\nabla^2 v$ . Integration by parts yields

$$\frac{d}{dt} \int_{\Omega_\Delta} \frac{1}{2} \|\nabla v\|^2 dx = -\nu \int_{\Omega_\Delta} \|\nabla^2 v\|^2 dx + \int_{\Omega_\Delta} ( (v \cdot \nabla)v \cdot \nabla^2 v - \nu_e \|\nabla^2 v\|^2 ) dx, \quad (2.4)$$

where  $\nu_e$  is assumed to be constant in  $\Omega_\Delta$ . As remarked above, the boundary terms that result from the integration by parts vanish because  $\Omega_\Delta$  is a periodic box. Thus we see that Eq. (2.3) holds if

$$\nu_e \int_{\Omega_\Delta} \|\nabla^2 v\|^2 dx = \int_{\Omega_\Delta} (v \cdot \nabla)v \cdot \nabla^2 v dx. \quad (2.5)$$

Chae (2005) showed that, for a periodic box, the right-hand side of Eq. (2.5) is equal to  $4 \int_{\Omega_\Delta} r(v) dx$ , where  $r(v) = -\frac{1}{3} \text{tr}(S^3(v)) = -\det S(v)$  is an invariant of the rate of strain tensor  $S(v)$ . It may be remarked here that the calculations by Chae are done for the 3D Euler equations; yet one can add the viscous term to each step of his calculations. The other nonzero invariant of  $S(v)$ ,  $q(v) = \frac{1}{2} \text{tr}(S^2(v))$ , has the property that  $4 \int_{\Omega_\Delta} q(v) dx = \int_{\Omega_\Delta} \|\nabla \times v\|^2 dx$  (see again Chae 2005). Since  $\nabla^2 v = -\nabla \times \omega$  with  $\omega = \nabla \times v$ , it follows that Eq. (2.5) is equivalent to

$$\nu_e \int_{\Omega_\Delta} q(\omega) dx = \int_{\Omega_\Delta} r(v) dx. \quad (2.6)$$

In conclusion, the eddy-viscous damping in Eq. (2.4) counteracts the nonlinear production in Eq. (2.4) if the eddy viscosity is taken according to Eq. (2.6). A noticeable difference between this result and the standard Smagorinsky model with a constant coefficient  $C_S$  is that the standard model depends only on the invariant  $q(v)$ , i.e., not on  $r$ .

The role of the invariant  $r(v)$  can be explained with the help of the vorticity  $\omega$ . By taking the curl of Eq. (1.2) we find the vorticity equation and from that we obtain that the enstrophy is governed by

$$\frac{d}{dt} \int_{\Omega_\Delta} \frac{1}{2} \|\omega\|^2 dx = \int_{\Omega_\Delta} \omega \cdot S\omega dx - (\nu + \nu_e) \int_{\Omega_\Delta} \|\nabla \omega\|^2 dx.$$

In the right-hand side we recognize the vortex stretching term that can produce smaller scales of motion and the dissipative term that should counteract the production of smaller scales at the scale  $\Delta$ . Now, Eq (2.6) leads to

$$\nu_e \int_{\Omega_\Delta} \|\nabla \omega\|^2 dx = \nu_e \int_{\Omega_\Delta} 4q(\omega) dx \stackrel{(2.6)}{=} \int_{\Omega_\Delta} 4r(v) dx = \int_{\Omega_\Delta} \omega \cdot S\omega dx.$$

Notice that the latter equality shows that  $r(v)$  is a measure for the vortex stretching (Chae 2005). Thus, Eq. (2.6) can also be interpreted as follows: the eddy viscosity is taken such that the corresponding damping of the enstrophy,  $\nu_e \int_{\Omega_\Delta} \|\nabla \omega\|^2 dx$ , equals the production by means of the vortex stretching mechanism,  $\int_{\Omega_\Delta} \omega \cdot S\omega dx$ . In other words, the eddy viscosity prevents the intensification of vorticity at the scale  $\Delta$  set by the map  $u \mapsto \bar{u}$ .

The dissipative term in Eq. (2.6) can be bounded in terms of the velocity. Indeed, with the help of Poincaré's inequality we get

$$\int_{\Omega_\Delta} q(\omega) dx = \int_{\Omega_\Delta} \frac{1}{4} \|\nabla \omega\|^2 dx \geq \frac{1}{C_\Delta} \int_{\Omega_\Delta} \frac{1}{4} \|\omega\|^2 dx = \frac{1}{C_\Delta} \int_{\Omega_\Delta} q(v) dx,$$

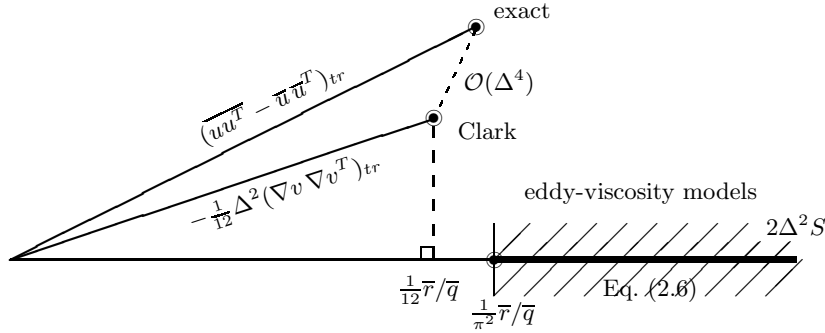


FIGURE 1. Some LES-models in the space of symmetric 3x3 tensors.

where the equality-sign holds if  $\omega$  is fully aligned with the eigenfunction of the dissipative operator  $-\nabla^2$  on  $\Omega_\Delta$  that is associated with the lowest (non-zero) eigenvalue. Hence, the eddy-viscous term in Eq. (2.6) dominates the nonlinear, convective term if

$$\nu_e \int_{\Omega_\Delta} q(v) dx \geq C_\Delta \int_{\Omega_\Delta} r(v) dx \quad (2.7)$$

or, stated otherwise,  $\nu_e \overline{q(v)} \geq C_\Delta \overline{r(v)}$ . This condition ensures that subfilter scales are dynamically insignificant, meaning that their energy is bounded by Eq. (2.1) where the upper bound decays at least as fast as  $\exp(-2\nu t/C_\Delta)$ , for any filter length  $\Delta$ .

### 3. Modeling consistency

It has not been established, thus far, that the choice of the minimal eddy viscosity

$$\nu_e = C_\Delta \overline{r(v)/q(v)} \quad (3.1)$$

will adequately model the subfilter contributions to the evolution of the filtered velocity. From the filtered Navier-Stokes solution  $\bar{u}$ , we can analyze the consistency of the eddy-viscosity model  $(\bar{u}\bar{u}^T - uu^T)_{tr} \approx 2\nu_e S(\bar{u})$  by *a priori* testing. Here we consider the traceless part (defined by  $A_{tr} = A - \frac{1}{3}\text{tr}(A)I$ ), because the trace of  $\bar{u}\bar{u}^T - uu^T$  can be incorporated into the pressure. A series expansion gives  $(\bar{u}\bar{u}^T - uu^T)_{tr} = -\frac{\Delta^2}{12}(\nabla\bar{u}\nabla\bar{u}^T)_{tr} + \mathcal{O}(\Delta^4)$ . The leading term is known as the Clark model. Unfortunately, the Clark model cannot be used as a stand-alone LES model, since it produces a finite time blow-up of the kinetic energy (Vreman *et al.* 1996). In other words, the Clark model can produce length-scales smaller than  $\Delta$ . Projecting both Eq. (3.1) and the Clark model onto  $S(v)$  yields

$$2C_\Delta \frac{\bar{r}}{\bar{q}} \int_{\Omega_\Delta} S(v) : S(v) dx = -\frac{\Delta^2}{12} \int_{\Omega_\Delta} (\nabla v \nabla v^T)_{tr} : S(v) dx. \quad (3.2)$$

The integral in the right-hand side equals  $-4 \int_{\Omega_\Delta} r(v) dx$  (Chae 2005). This shows that  $r$  provides a measure of the alignment of the Clark model and  $S$ . By definition we have  $S : S = 2q$ . Consequently, Eq. (3.2) shows that the order of the modeling error is optimal if  $C_\Delta = \Delta^2/12$ . This value is in fair agreement with the Poincaré constant,  $C_\Delta = \Delta^2/\pi^2$ ; yet, it is slightly lower. The overall situation is sketched in Figure 1. The horizontal axis in this figure represents all possible eddy-viscosity models; the axis is parameterized by the eddy viscosity. The shaded part of the horizontal axis in Figure 1 depicts the subset of eddy viscosities that satisfy Eq. (2.6). The projection of the Clark model onto

the horizontal axis falls outside the shaded area; hence it cannot be guaranteed that this projection damps subfilter scales adequately. This reflects that the Clark model can produce subfilter scales. Eq. (3.1) forms the best approximation of the projection of the Clark model provided the eddy-viscosity model is restricted by Eq. (2.6). The projection onto  $S(v)$  is chosen to evaluate the dissipation provided by these models.

Furthermore, Eq. (3.1) yields  $\nu_e = 0$  in any laminar (part of the) flow since  $r = 0$  in laminar flow. At a no-slip wall  $r = 0$  too; hence  $\nu_e = 0$  at the wall. In homogeneous, isotropic turbulence, we have  $r/q \propto Re^{1/2}$ . Therefore,  $\nu_e/\nu \propto Re^{3/2}$  for fixed  $\Delta$ . Additionally, we obtain that  $\nu_e + \nu \rightarrow \nu$  if  $\nu \propto Re^{-1} \propto \Delta^2 r/q \propto \Delta^2 Re^{1/2}$ , that is, if  $\Delta \propto Re^{-3/4}$ . This shows that the eddy viscosity given by Eq. (3.1) vanishes as  $\Delta$  is of the order of  $Re^{-3/4}$ , i.e., if  $\Delta$  approaches the Kolmogorov scale.

#### 4. Towards a dynamic model

We decompose  $v$  with the help of the filter into  $v = \bar{v} + v'$ . The residual  $v'$  represents the behavior of the large-eddy solution  $v$  within the filter-box  $\Omega_\Delta$ . This part of  $v$  is needed to compute the eddy viscosity directly from Eq. (3.1), i.e., to compute the ratio of  $\overline{r(v)}$  and  $\overline{q(v)}$ . Here, we cannot simply take  $\overline{q(v)} = q(\bar{v})$ , because the relation between  $q$  and  $v$  is nonlinear (similarly for  $r$ ). This problem is similar to the closure problem in LES, except that the original closure problem concerns the residual of the Navier-Stokes solution  $u$ , whereas here it is about the residual of the large-eddy solution  $v$ .

To start, we assume that the grid is chosen such that residual  $v'$  of the solution of Eq. (1.2) can be resolved numerically. Obviously, this implies that the grid size is taken to be smaller than the filter width  $\Delta$ . The eddy viscosity can then be computed directly from Eq. (2.6). This approach is tested for decaying isotropic turbulence.

The decaying isotropic turbulence of Comte-Bellot & Corrsin (1971) (denoted as CBC hereinafter) is chosen for the test case. It was experimentally generated using the grid turbulence with the mesh size of  $M$  (=5.08 cm) and the free-stream velocity of  $U_0$  (= 10 m/s). The Taylor micro-scale Reynolds number is  $Re_\lambda = u_{rms}\lambda/\nu = 71.6$  at  $tU_0/M=42$ . The filtered Navier-Stokes equations are solved using a dealiased spectral code. For time integration, a second-order semi-implicit scheme is used: diffusion terms are treated implicitly using the Crank-Nicolson method and a third-order Runge-Kutta scheme is applied to convection terms. A divergence-free initial field at  $tU_0/M=42$  is generated using the rescaling method (Kang *et al.* 2003). All the simulations are conducted at the resolution of  $32^3$  in a computational cube of  $(11M)^3$ . In the present approach based on Eq. (2.6), the absolute value of  $r(v)$  is used for the determination of  $\nu_e$ . That is,  $\nu_e$  is obtained as

$$\nu_e = \frac{\int_{\Omega_\Delta} |r(v)| dx}{\int_{\Omega_\Delta} q(\omega) dx}. \quad (4.1)$$

In the present study, the eddy viscosity model with Eq. (4.1) is denoted as the  $rq$  model.

Figure 2 shows the three-dimensional (3D) energy spectra at  $tU_0/M=42, 98$  and 171 and the temporal evolution of the resolved kinetic energy with the  $rq$  model. The energy spectra are non-dimensionalized by  $L_{ref} = 11M/2\pi$  and  $u_{ref} = \sqrt{3/2} u_{rms}|_{tU_0/M=42}$ . For the integration of the invariants  $r$  and  $q$ , two different local volumes are tested:  $\Omega_\Delta = (2\Delta)^3$  and  $\Omega_\Delta = (4\Delta)^3$ . As shown in Figure 2, results from LES with the  $rq$  model are in excellent agreement with the experimental data of CBC. Note that the results from the  $rq$  model with  $\Omega_\Delta = (2\Delta)^3$  and  $\Omega_\Delta = (4\Delta)^3$  are almost the same, showing that the performance of the  $rq$  model is not very sensitive to the choice of local volume  $\Omega_\Delta$ .

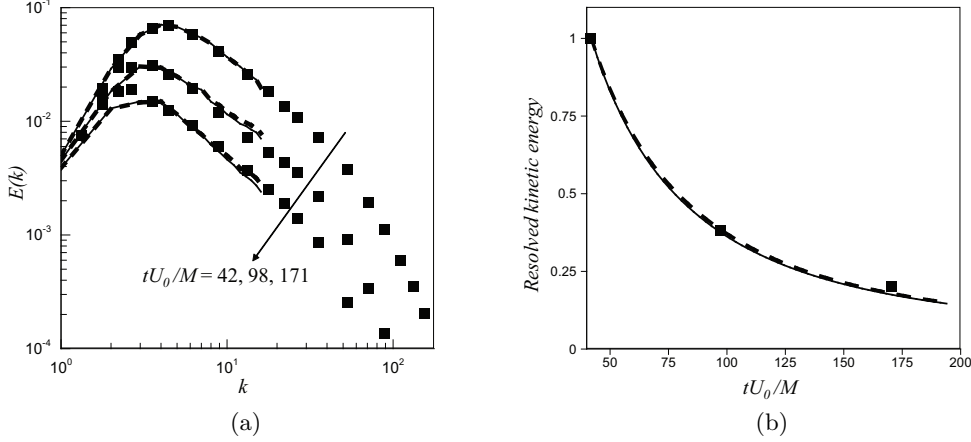


FIGURE 2. Results from LES of the decaying isotropic turbulence of CBC with  $rq$  model: (a) three-dimensional energy spectra at  $tU_0/M=42, 98, 171$ ; (b) temporal evolutions of the resolved kinetic energy. ■, CBC; —,  $rq$  model with  $\Omega_\Delta = (2\Delta)^3$ ; — —,  $rq$  model with  $\Omega_\Delta = (4\Delta)^3$ .

Next, we take the grid width equal to the filter width  $\Delta$ ; hence, the subfilter part  $v'$  of the solution  $v$  cannot be computed numerically. In a finite volume approximation, for instance, we resolve only  $\bar{v}$  if the grid size is taken equal to  $\Delta$ , cf. Schumann (1975). In this case, the subfilter part of the ratio of  $r(v)$  and  $q(v)$  in Eq. (3.1) is to be modelled. In other words, the part lost in the filtering process is to be represented by an appropriate model. In this paper, we base our model on the mean value theorem for integration. This theorem states that there exists a point  $\xi$  in  $\Omega_\Delta$  such that

$$\nu_e = C_\Delta \frac{\int_{\Omega_\Delta} r^{1/3}(v) r^{2/3}(v) dx}{\int_{\Omega_\Delta} q(v) dx} = C_\Delta r^{1/3}(\hat{v}) \frac{\int_{\Omega_\Delta} r^{2/3}(v) dx}{\int_{\Omega_\Delta} q(v) dx},$$

where  $\hat{v} = v(\xi, t)$ . Here it may be remarked that  $r^{2/3}$  and  $q$  are continuous functions that do not change sign in  $\Omega_\Delta$ . Furthermore, the three roots of the characteristic polynomial of  $S(v)$  must be real-valued because  $S(v)$  is symmetric. This requirement leads to the constraint  $27r^2 \leq 4q^3$ , everywhere in  $\Omega_\Delta$ . Consequently, if we assume that  $r^{1/3}$  has only modest variations within  $\Omega_\Delta$ , that is  $r^{1/3}(\hat{v}) \approx r^{1/3}(v)$ , we arrive at the condition

$$\nu_e \leq C_\Delta (4/27)^{1/3} |r(v)|^{1/3}, \quad (4.2)$$

with  $C_\Delta = \Delta^2/\pi^2$ . To refine the subfilter modelling, we replace the constant in (4.2) by a coefficient that is computed dynamically. That is, we take

$$\nu_e = C \Delta^2 |r(v)|^{1/3}, \quad (4.3)$$

where the coefficient  $C$  is computed in a manner proposed by Germano *et al.* (1991). The absolute value of  $r(v)$  is taken to ensure that the eddy viscosity is non-negative (assuming  $C > 0$ ). Further development could consider not using the absolute value in order to allow backscatter. Now, the coefficient  $C$  in Eq. (4.3) is determined based on the procedure of dynamic global model using the Germano identity (Park *et al.* 2006; Lee *et al.* 2010):

$$C = -\frac{1}{2} \frac{\langle L_{ij} M_{ij} \rangle_V}{\langle M_{ij} M_{ij} \rangle_V}, \quad (4.4)$$

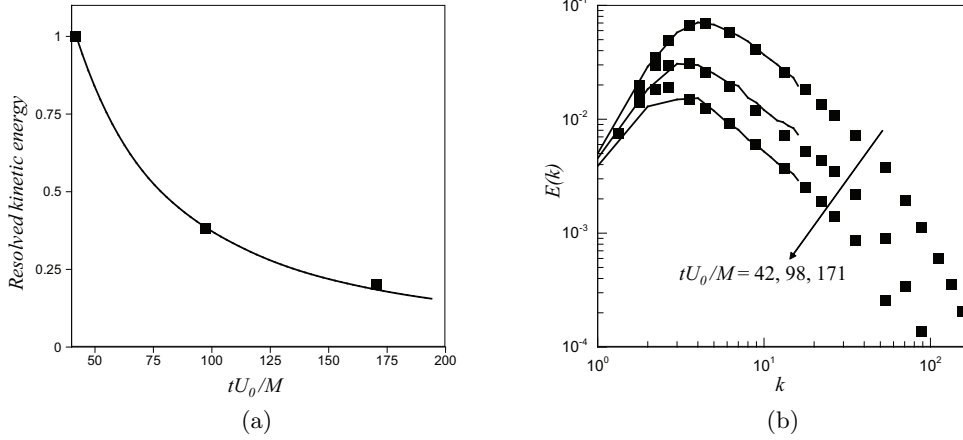


FIGURE 3. Results from LES of the decaying isotropic turbulence of CBC with the  $|r|^{1/3}$  model: (a) three-dimensional energy spectra at  $tU_0/M=42, 98, 171$ ; (b) temporal evolutions of the resolved kinetic energy.  $\blacksquare$ , CBC; —,  $|r|^{1/3}$  model.

where

$$L_{ij} = \widetilde{\tilde{u}_i \tilde{u}_j} - \tilde{u}_i \tilde{u}_j, \quad (4.5)$$

$$M_{ij} = \tilde{\Delta}^2 |r(\tilde{v})|^{1/3} \tilde{S}_{ij} - \Delta^2 |r(v)|^{1/3} \tilde{S}_{ij}. \quad (4.6)$$

Here,  $\tilde{(\cdot)}$  denotes the test-filtering operation,  $\tilde{\Delta} = 2\Delta$ , and  $\langle \bullet \rangle_V$  denotes the instantaneous volume averaging over the computational domain. The test filter used is also a top-hat filter as was previously assumed. This model coefficient  $C$  is constant in space but varies in time. In the next section, this approach is tested for decaying isotropic turbulence and turbulent channel flow.

## 5. Results

### 5.1. Decaying isotropic turbulence

The decaying isotropic turbulence of CBC described in the previous section is examined using the  $|r|^{1/3}$  model. Figure 3 shows the temporal evolution of the resolved kinetic energy and the 3D energy spectra. As shown, the present subgrid-scale model accurately predicts the experimental data of CBC. Figure 4 shows the temporal evolution of the model coefficient  $C$  in Eq. (4.4). The model coefficient is nearly constant, agreeing with Eq. (4.2). The present result indicates that the  $|r|^{1/3}$  model together with a dynamic global approach is capable of predicting transient turbulent flows.

### 5.2. Turbulent channel flow

Numerical simulations of an  $Re_\tau = 590$  channel flow are performed using a fourth-order, conservative finite difference code based on the numerics of Morinishi *et al.* (1998). Temporal integration is performed using a mixed Runge-Kutta/Crank-Nicholson scheme (Spalart *et al.* 1991), where the wall-normal diffusion terms are treated implicitly. Simulations are performed on a  $64 \times 64 \times 64$  grid corresponding to a  $\Delta x^+ \approx 58$  and  $\Delta z^+ \approx 29$ . The grid is stretched in the wall-normal direction with a  $\Delta y^+ = 0.4$  at the channel wall

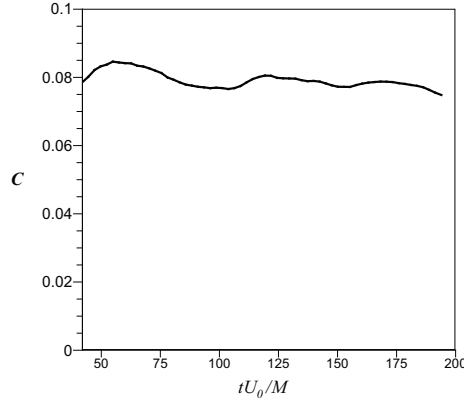


FIGURE 4. Temporal evolution of the model coefficient  $C$  [Eq. (4.4)] for decaying isotropic turbulence of CBC.

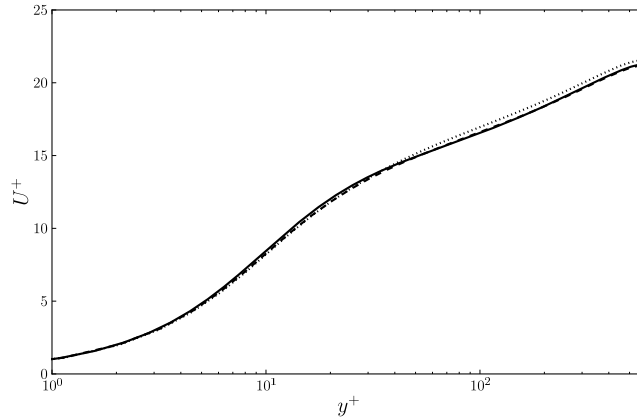


FIGURE 5. Mean velocity profiles for turbulent channel flow at  $Re_\tau = 590$  using  $64^3$  grid points using the dynamic  $|r|^{1/3}$  model (---) and the dynamic Smagorinsky model ( $\cdots$ ). Solid line denotes the DNS of Moser *et al.* (1999).

and  $\Delta y^+ = 50$  at the channel centerline. The model coefficient,  $C = C(y)$ , is computed dynamically and is allowed to vary with the distance from the channel walls. Results are compared with the dynamic Smagorinsky model (Germano *et al.* 1991; Lilly 1992) and with the filtered DNS of Park *et al.* (2006).

Figure 5 shows the mean velocity profiles for the simulations using the dynamic  $|r|^{1/3}$  model, the dynamic Smagorinsky model, and the filtered DNS. The  $|r|^{1/3}$  model shows excellent agreement with the DNS mean velocity profile. At this Reynolds number and resolution, the  $|r|^{1/3}$  model is only slightly better than the dynamic Smagorinsky, and both models perform adequately. Figure 6 depicts the root mean square (rms) fluctuations of the velocity components. Near the wall, the  $|r|^{1/3}$  model better predicts the filtered DNS quantities, with markedly better predictions in the wall normal and spanwise ve-

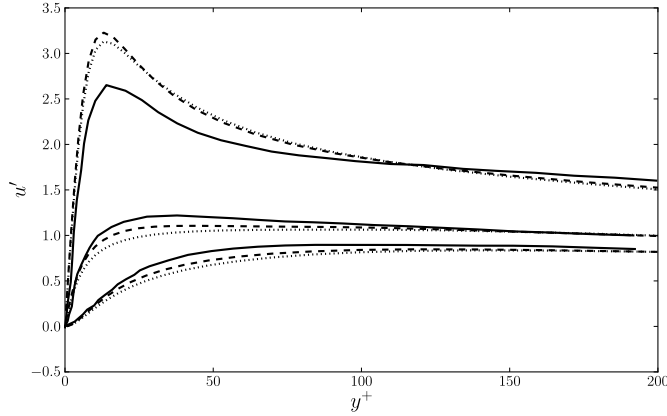


FIGURE 6. Rms velocity profiles for turbulent channel flow at  $Re_\tau = 590$  using  $64^3$  grid points using the dynamic  $|r|^{1/3}$  model (---) and the dynamic Smagorinsky model ( $\cdots$ ). Solid line denotes the filtered DNS of Park *et al.* (2006).

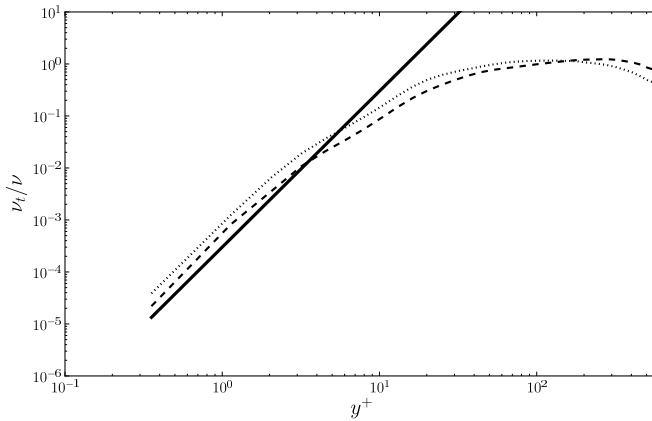


FIGURE 7. Mean eddy viscosity normalized by the physical viscosity for the dynamic  $|r|^{1/3}$  model (---) and the dynamic Smagorinsky model ( $\cdots$ ) shown in log scale for an  $Re_\tau = 590$  channel flow. Solid line denotes  $y^{+3}$  behavior.

locity components. Beyond  $y^+ = 200$ , the two models are virtually indistinguishable in their predictions of rms quantities. Figure 7 shows the ensemble averaged eddy viscosity (normalized by the physical viscosity),  $\nu_t$ , for the different models. Through the use of the dynamic procedure, the  $|r|^{1/3}$  correctly captures the expected  $y^3$  behavior near the wall. Additionally, the  $|r|^{1/3}$  produces more eddy viscosity near the channel centerline and its peak mean eddy viscosity occurs much further from the wall ( $y^+ \approx 300$ ) when compared to the dynamic Smagorinsky model ( $y^+ \approx 100$ ). It has been documented that the peak eddy viscosity for the Smagorinsky model typically scales with the viscous wall units, but it is unclear from this numerical experiment whether that behavior will hold for the dynamic  $|r|^{1/3}$  model.

## 6. Concluding remarks

A new, dynamic eddy viscosity model has been presented above that shows good predictions of decaying isotropic turbulence and turbulent channel flow. The model is derived systematically from the requirement that the eddy viscosity should damp all scales smaller than the filter width,  $\Delta$ . Further investigation of the performance of this model in other flow configurations is needed.

## REFERENCES

- CHAE, D. 2005 On the spectral dynamics of the deformation tensor and a new a priori estimates for the 3D Euler equations. *Communications in Mathematical Physics* **263**, 789–801.
- COMTE-BELLOT, G. & CORRISIN, S. 1971 Simple Eulerian time correlation of full- and narrow-band velocity signals in grid-generated, ‘isotropic’ turbulence. *Journal of Fluid Mechanics* **48**, 273–337.
- GERMANO, M., PIOMELLI, U., MOIN, P. & CABOT, W. 1991 A dynamic subgrid-scale eddy viscosity model. *Physics of Fluids A* **3**, 1760.
- KANG, H. S., CHESTER, S. & MENEVEAU, C. 2003 Decaying turbulence in an active-grid-generated flow and comparisons with large-eddy simulation. *Journal of Fluid Mechanics* **480**, 129–160.
- LEE, J., CHOI, H. & PARK, N. 2010 Dynamic global model for large eddy simulation of transient flow. *Physics of Fluids* **22**, 075106.
- LILLY, D. 1992 A proposed modification of the Germano subgrid-scale closure method. *Physics of Fluids A* **4**, 633.
- MORINISHI, Y., LUND, T., VASILYEV, O., & MOIN, P. 1998 Fully conservative higher order finite difference schemes for incompressible flow. *Journal of Computational Physics* **143**, 90–124.
- MOSER, R., KIM, J. & MANSOUR, N. 1999 Direct numerical simulation of turbulent channel flow up to  $Re_\tau = 590$ . *Physics of Fluids* **11**, 943.
- PARK, N., LEE, S., LEE, J. & CHOI, H. 2006 A dynamic subgrid-scale eddy viscosity model with a global model coefficient. *Physics of Fluids* **18**, 125109.
- PAYNE, L. & WEINBERGER, H. F. 1960 An optimal Poincaré inequality for convex domains. *Archive for Rational Mechanics and Analysis* **5**, 286–292.
- SCHUMANN, U. 1975 Subgrid scale model for finite difference simulations of turbulent flows in plane channels and annuli. *Journal of Computational Physics* **18**, 376–404.
- SPALART, P., MOSER, R. & ROGERS, M. 1991 Spectral methods for the Navier-Stokes equations with one infinite and two periodic directions. *Journal of Computational Physics* **96**, 297–324.
- VREMAN, B., GEURTS, B. & KUERTEN, H. 1996 Large-eddy simulation of the temporal mixing layer using the Clark model. *Theoretical and Computational Fluid Dynamics* **8**, 309–324.